International Journal of Astrobiology 8 (4): 291–300 (2009) Printed in the United Kingdom
doi:10.1017/S1473550409990231

Effect of thenardite on the direct detection of aromatic amino acids: implications for the search for life in the solar system

C. Doc Richardson[1], Nancy W. Hinman[1] and Jill R. Scott[2]

[1]*Geosciences Department, University of Montana, Missoula, 32 Campus Drive #1296, Missoula, MT 59812, USA*
[2]*Chemical Sciences, Idaho National Laboratory, 1765 North Yellowstone Hwy, Idaho Falls, ID 83415, USA*
e-mail: Jill.Scott@inl.gov

Abstract: With the discovery of Na-sulphate minerals on Mars and Europa, recent studies using these minerals have focused on their ability to assist in the detection of bio/organic signatures. This study further investigates the ability of thenardite (Na_2SO_4) to effectively facilitate the ionization and identification of aromatic amino acids (phenylalanine, tyrosine and tryptophan) using a technique called geomatrix-assisted laser desorption/ionization in conjunction with a Fourier transform ion cyclotron resonance mass spectrometry. This technique is based on the ability of a mineral host to facilitate desorption and ionization of bio/organic molecules for detection. Spectra obtained from each aromatic amino acid alone and in combination with thenardite show differences in ionization mechanism and fragmentation patterns. These differences are due to chemical and structural differences between the aromatic side chains of their respective amino acid. Tyrosine and tryptophan when combined with thenardite were observed to undergo cation-attachment ($[M+Na]^+$), due to the high alkali ion affinity of their aromatic side chains. In addition, substitution of the carboxyl group hydrogen by sodium led to formation of $[M\text{-}H+Na]Na^+$ peaks. In contrast, phenylalanine mixed with thenardite showed no evidence of Na^+ attachment. Understanding how co-deposition of amino acids with thenardite can affect the observed mass spectra is important for future exploration missions that are likely to use laser desorption mass spectrometry to search for bio/organic compounds in extraterrestrial environments.

Received 13 March 2009, accepted 21 July 2009, first published online 28 August 2009

Key words: aromatic amino acids, biosignature, Europa, FTICR-MS, GALDI, geomatrix, Mars, thenardite.

Introduction

Both hydrated and unhydrated Na-sulphate minerals exist in numerous bodies throughout the solar system. On Earth, Na-sulphates form in non-marine environments (playas, sabkhas), in basaltic weathering (Karlo *et al*. 1980; Hill & Forti 1997), as fumarolic exhalations (Hill & Forti, 1997), in atmospheric aerosols (Rankin *et al*. 2002), and in subsurface Antarctic ice (Ohno *et al*. 2006). Beyond Earth, Na-sulphates are found on Mars as weathering products in evaporitic environments (Zhu *et al*. 2006; Mangold *et al*. 2008), and as surface components of the Jupiter moons Ganymede (McCord *et al*. 2001), Io (Wiens *et al*. 1997), and Europa (McCord *et al*. 1998; McCord *et al*. 1999; Johnson 2000). Additionally, numerous prebiotic organic compounds have been detected on these Solar bodies, making them high priority candidates for biological activity (Kotler *et al*. 2009). Thus, with the ubiquity of Na-sulphates in the Solar System, understanding their ability to preserve and relinquish bio/organic signatures, which are signatures that are organic and potentially biological in origin, is crucial in the search for extraterrestrial life.

Since the *Viking* missions (Klein 1979; Oro 1979), the search for life in the Solar System has predominantly focused on the planet Mars (Chyba & McDonald 1995). Unfortunately, due to the oxidizing Martian atmosphere, bio/organic compounds are better preserved when protected (via substitution, inclusion, adsorption) by a mineral host to avoid degradation (Parnell *et al*. 2007). On Earth, organic compounds are often co-deposited in sulphate salts during mineralization (Aubrey *et al*. 2006; Kotler *et al*. 2008; Richardson *et al*. 2008). Likewise, if life once existed on Mars, bio/organic compounds could be incorporated and preserved in the Martian geological record. Sulphate minerals are a likely candidate for bio/organic preservation, since they are ubiquitous on the Martian regolith, forming in evaporitic environments due to weathering of primary basaltic minerals (Squyres *et al*. 2004). Chemical/mineralogical models using data from SNC-type meteorites, Mars Exploration Rovers and Martian orbiters provide evidence that Na-sulphates are

a likely constituent of evaporitic assemblages on Mars (Tosca & McLennan 2006). Additionally, spectrometry data from the Visible and Infrared Mineralogical Mapping Spectrometer (OMEGA) aboard the Mars *Express* orbiter, detected signatures consistent with the presence of thenardite (Na_2SO_4) near the low-albedo region of Syrtis Major (Zhu *et al*. 2006). More recently, Mangold *et al*. (2008) suggested that polyhydrated Na-sulphates may be a constituent in the layered sulphate sequences of West Candor Chasma, known to contain one of the largest sequences of sulphate minerals on Mars.

In addition to Mars, several Galilean satellites have spectrometric signatures characteristic of surficial Na-sulphates. Of these satellites, the moon-sized satellite of Jupiter, Europa, is the most promising in the search for extraterrestrial life, as it probably contains liquid water, biogenic elements and chemical disequilibria (Gaidos *et al*. 1999; Kargel *et al*. 2000; Chyba & Phillips 2002; Chela-Flores 2006). The surface composition of Europa is dominated by water ice with localized regions of non-ice components, consisting mostly of polyhydrated Na- and Mg-sulphate species (McCord *et al*. 1998; McCord *et al*. 1999; Kargel *et al*. 2000; Fanale *et al*. 2001; Zolotov & Shock 2001). These sulphate minerals originate as solutes in the internal ocean, probably derived from leaching and degassing of elements on the ocean-rock interface (Fanale *et al*. 2001). These solutes subsequently are emplaced on the surface by cryovolcanism and impact events (Orlando *et al*. 2005).

Geomatrix-assisted laser desorption/ionization mass spectrometry (GALDI-MS) is a proven technique capable of characterizing bio/organic compounds associated with terrestrial sulphate minerals (Kotler *et al*. 2008; Richardson *et al*. 2008), and possibly bio/organic compounds associated with returned samples from Mars and Europa. This technique uses a mineral matrix to aid in desorption so that organic signatures can be detected along with any bio/organic signatures present in the sample (Yan *et al*. 2007b). Further, the mineral matrix can stabilize organic ions to aid detection. Thus, the ability of minerals to facilitate the ionization and desorption of bio/organic compounds is a primary focus in the effectiveness of GALDI-MS. When used in conjunction with a Fourier transform ion cyclotron resonance mass spectrometer (FTICR-MS) (Scott & Tremblay 2002), GALDI-FTICR-MS has the ability to obtain high-resolution spectra using a single laser shot, with low detection limits for chemical signatures, with little or no sample preparation (Yan *et al*. 2007a; Kotler *et al*. 2008; Richardson *et al*. 2008). When coupled with imaging or mapping capability (Scott & Tremblay 2002), GALDI-FTICR-MS can search for bio/organic signatures in heterogeneous geomatrices from both terrestrial samples (Kotler *et al*. 2008; Richardson *et al*. 2008) and future samples returned from Mars and Europa. While FTICR-MS systems are not practical for a rover, a low-power, compact laser desorption quadrupole ion trap mass spectrometer is being developed for deployment on Mars as part of the Mars Organic Molecule Analyzer as part of the ExoMars mission (Evans-Nguyen *et al*. 2008).

Previous GALDI-FTICR-MS investigations have focused on sulphate salts and halides (NaCl) acting as mineral matrices to facilitate the ionization and desorption of bio/organic compounds (fatty acids, amino acids and proteins) (Yan *et al*. 2007a,b; Kotler *et al*. 2008; Richardson *et al*. 2008). These combinations produced inorganic and organic cluster ions (Kotler *et al*. 2008; Richardson *et al*. 2008), deprotonated bio/organic compounds ($[M\text{-}H]^-$) (Richardson *et al*. 2008) and/or cation-attached peaks $[M+Na]^+$ (Yan *et al*. 2007a). Polycyclic aromatic hydrocarbon (PAH) compounds are also of interest due to their occurrence throughout the universe, including meteorites (Kotler *et al*. 2009). Unlike most bio/organic compounds, PAH compounds self-ionize during laser ablation and may facilitate the detection of non-ionizing bio/organic compounds (Yan *et al*. 2007b).

The occurrence of thenardite throughout the solar system makes it a primary candidate for GALDI-FTICR-MS studies. The mineral has sufficient gas-phase basicity to abstract a proton from the aliphatic amino acid glycine, contrary to results using other sulphate salts (Richardson *et al*. 2008). Furthermore, thenardite taken from a terrestrial evaporitic environment showed signatures consistent with bio/organic compounds (Richardson *et al*. 2008). Gas-phase reactions between thenardite and stearic acid produce organic and inorganic cluster ions, similar to cluster ions observed by matrix-assisted laser desorption/ionization (MALDI), such as an accumulation of adducts (Karas & Hillenkamp 1988), matrix moieties (Knochenmuss *et al*. 1996) and/or analyte components (Ham *et al*. 2003; Budimir *et al*. 2007). Thenardite was also used to ascertain the limit of detection for GALDI-FTICR-MS, estimated to be approximately three parts per trillion based on bulk concentrations, corresponding into $\sim$7 zeptomoles (10^{-21}) per laser shot (Richardson *et al*. 2008).

In this study, we evaluate the ability of thenardite to facilitate the desorption, ionization and detection of aromatic amino acids using GALDI-FTICR-MS. Aromatic compounds were chosen because they have been proposed as primary biosignature targets in the solar system (Storrie-Lombardi *et al*. 2001; McKay 2007; Parnell *et al*. 2007), as they readily donate electrons via multiple metabolic pathways during protein synthesis in terrestrial microorganisms (Porat *et al*. 2004; Plekan *et al*. 2008). Spectra obtained from mixing of individual aromatic amino acids (tryptophan, tyrosine and phenylalanine) with thenardite were evaluated for differences in ionization and fragmentation patterns. The effectiveness of thenardite to assist in the detection of aromatic amino acids and other bio/organic signatures, along with its occurrence on Mars and Europa, further signifies its importance in the search for life in the solar system.

Materials and methods

Physical mixtures of thenardite (Fischer Scientific, Pittsburgh, PA) with phenylalanine, tyrosine and tryptophan (Sigma-Aldrich, St. Louis, MO) were prepared following the methods of Richardson *et al*. (2008) and Yan *et al*. (2007a).

https://doi.org/10.1017/S1473550409990231 Published online by Cambridge University Press

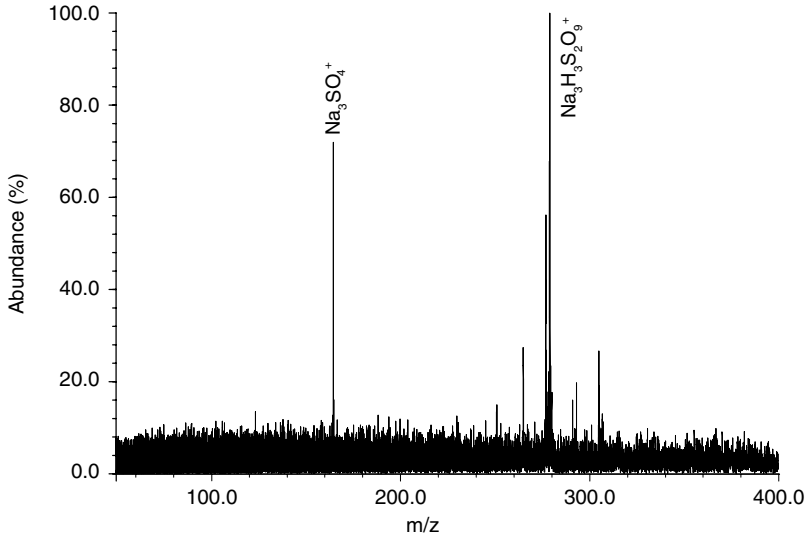

Fig. 1. Positive ion GALDI-FTICR-MS spectrum of thenardite.

Approximately 1×10^{-4} mole (0.02 g) of tryptophan was added to 10 g of thenardite. The mixture was then mixed for approximately 5 min at 70 Hz using a vortex mixer (Model 231, Fischer Scientific, Pittsburgh, PA) with two 4.5 mm zinc-plated steel ball bearings (Premium Grade BBs, Daisy Outdoor Products, Rogers, AR) to ensure a relatively homogeneous sample corresponding to a bulk concentration of approximately 2 ppm. The phenylalanine and tyrosine samples were produced in a similar manner to that of tryptophan.

Lower concentrations of phenylalanine, tyrosine and tryptophan with thenardite were produced by a series of dry serial dilutions with incremental steps of 10^{-3} molar. The resulting samples had an approximate concentration of 1 nM (approximately 3 ppb). Vortex mixing was completed between all dilutions steps to ensure homogeneity, similar to previous methods by Richardson *et al.* (2008) and Yan *et al.* (2007a). Samples were then pressed into half-inch pellets using a Beckman dye with a Carver Laboratory Press (Menomonee Falls, WI) at an approximate pressure of 3.5×10^{-7} Pa. Samples were subsequently mounted on copper discs using epoxy (Devcon 5 minute epoxy, Danvers, MA). To prevent absorption of the epoxy, the epoxy was allowed to dry for approximately 5 min before applying the sample pellet.

Instrumentation

Mass spectra were obtained using a laboratory-built imaging laser desorption FTICR-MS (McJunkin *et al.* 2002; Scott & Tremblay 2002; Scott *et al.* 2003) with a 7 T Oxford (Oxford, England) superconducting magnet. Instrumental parameters are similar to those previously described (Yan *et al.* 2007a,b; Kotler *et al.* 2008; Richardson *et al.* 2008). Data acquisition was accomplished using an Odyssey control and data acquisition computer system (Finnigan FT/MS, Bremen, Germany). Desorption/ionization was performed using a Nd:YAG laser (Continuum, Santa Clara, CA) operating at 355 nm with a 6 ns laser pulse and an irradiance of 1×10^{8} W cm^{-2}, unless otherwise specified. During ionization, voltage potential between the front and back plates was maintained at 0 V, while after ionization, a trapping potential of 2 V was applied to both trap plates. A delay of 0.5 s was allowed prior to chirp excitation over the range of 50 Hz to 4 MHz (corresponding to m/z 10^5 and 26.9, respectively) with a sweep rate of 3600 Hz μs^{-1}. Ions were detected in direct mode using 128 K data points. After acquisition, data was baseline corrected, Hamming apodized, zero filled, and Fourier transformed. Pressure during analysis was at most 4×10^{-9} Torr. For the given parameters, the LD-FTICR-MS has a mass error of ± 0.003 Da, resolution of $\sim$10 000), high sensitivity ($\leq$400 ions for peaks with signal-to-noise ratio $\sim$3) for m/z range $<$2000 Da. All spectra were acquired with single laser shots and in the positive mode unless specified otherwise. Peak identification was accomplished by systematic analysis following the method described in Kotler *et al.* (2008). Additional information regarding FTICR-MS can be found in the literature (Comisarow 1993; Marshall *et al.* 1998; Marshall & Hendrickson 2002).

Results and discussion

The possibility of life on Mars and Europa in conjunction with the occurrence of endogenous Na-sulphates that could potentially harbour signatures of life makes understanding the interaction between Na-sulphates and bio/organic compounds crucial for the potential applications for laser desorption mass spectrometry (LDMS) techniques in the search for extraterrestrial life in the solar system. A first step towards understanding the spectra is distinguishing the difference between peaks produced from inorganic ions generated from the mineral and those of the bio/organic compounds of interest. The second major step is determining if the mineral is likely to affect the types of peaks observed from the bio/organic compounds, which is the primary focus of this paper.

Positive spectra of the mineral thenardite (Fig. 1) by itself are dominated by a small number of peaks. The peaks

https://doi.org/10.1017/S1473550409990231 Published online by Cambridge University Press

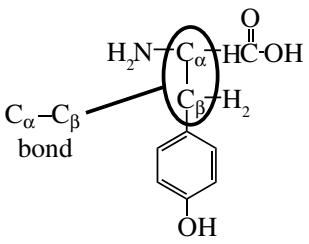

Fig. 2. The location of C_α—C_β bond in the aromatic amino acids, using Phe for illustration.

represent inorganic cluster ions at m/z 164, 265, 279 and 305. These peaks are easily identified as representing inorganic ions, based on their mass defect (Sack *et al*. 1984; McLafferty & Tureček 1993; Kim *et al*. 2006; Kotler *et al*. 2008). The high mass accuracy and resolution of FTICR-MS enables distinction between inorganic and organic ions. Detailed explanation and methodology for identification of peaks is found in Kotler *et al*. (2008) and Richardson *et al*. (2008). The presence of H, and some of the O, in the inorganic ions is likely to be the result of remnant water left behind from hydrated Na-sulphate mineral phases. Similar inorganic cluster ions have been previously reported in Na-sulphate spectra (Van Vaeck *et al*. 1998; Kotler *et al*. 2008; Richardson *et al*. 2008), including the $Na_3SO_4^+$ peak at m/z 164 observed by Van Vaeck *et al*. (1998). Unlike the negative mode spectra of thenardite which show numerous inorganic cluster ions (Richardson *et al*., 2008), the positive mode spectrum of thenardite (Fig. 1) shows significantly fewer peaks.

The aromatic amino acids are presented from lowest to highest molecular weight, which also corresponds with their cation affinities (i.e. Phe < Tyr < Trp). A common fragmentation occurs from the cleavage of the C_α—C_β bond (location of C_α—C_β bond in the aromatic amino acids is shown in Fig. 2, using Phe for illustration) for all of the aromatic amino acids (Plekan *et al*. 2008). The structural schemes in Figs 3, 4 and 5 are provided as an aid to understanding how the ions are related to the neutral amino acid and as possible formation pathways to the observed ions. They are not necessarily indicative of the actual gas-phase structure, which can be quite complex (McLafferty & Tureček 1993; El Aribi *et al*. 2004) and are beyond the scope of this paper.

The spectrum of phenylalanine alone (Fig. 3(a)) is dominated by fragmentation of the molecular backbone and the phenyl aromatic ring ion. Decarboxylation of the molecular backbone results in the peak at m/z 120. Further fragmentation is seen in the cleavage of the C_α—C_β bond of the molecular backbone resulting in the positively charged $C_2H_4NO_2^+$ fragmented backbone at m/z 74 and the phenyl ring fragment observed at m/z 91 (Fig. 3(c)). The high intensity peaks at m/z 155 and 139 in the phenylalanine spectrum (Fig. 3(a)) are due to sample contamination (< 1 %) of alkali ions (K^+, Na^+) and their subsequent gas-phase interactions. These contaminants may have been introduced via a salt with its own counter anion, or as a salt of phenylalanine. Regardless of the exact source of the contaminants, these cluster ions have inorganic compositions based on their high mass defects. Furthermore, systematic analysis of their isotopic distribution supports the presence of alkali elements and their subsequent interaction with the phenylalanine and thenardite moieties. Further, the peak at m/z 38.96 corresponds to singly charged K^+ ions. Alkali element contamination has been reported in similar spectra of aromatic amino acids (Karas *et al*. 1985; Willey *et al*. 1998; Plekan *et al*. 2008). The high intensity of the alkali element-attached peaks reflects the ease of alkali element ionization at 355 nm, resulting in abundant alkali element desorption and subsequent high intensity peaks (Karas *et al*. 1985; Scott *et al*. 2006; Yan *et al*. 2007b), although the exact formation mechanisms of these cluster ions are highly speculative and unclear at this time.

Excluding the alkali element-cluster peaks, the highest intensity peak in the phenylalanine spectrum (Fig. 3(a)) is caused by decarboxylation ($[M\text{-}COOH]^+$), contrary to studies by Plekan *et al*. (2008) whose major peak corresponded to breakage of the C_α—C_β bond and the subsequent formation of the molecular backbone ion. The difference in major peaks between studies is likely to be a function of the laser irradiance and system parameters. Major peaks corresponding to $[M\text{-}COOH]^+$ were observed using LDMS instrumentation (Karas *et al*. 1985) under higher laser intensities than were used in this study. High laser fluences could cause ablation at the laser–mineral interface rather than desorption (Aubriet *et al*. 2005; Aubriet 2007; Aubriet & Muller 2008). However, the distinction between desorption and ablation processes for GALDI-FTICR-MS has not been determined because only one type of spectral signature was observed when varying the laser irradiance. The relatively high laser irradiance used in GALDI-FTICR-MS appears to be necessary for optimal ionization due to the refractory nature of the host minerals.

The absence of peaks in mixed phenylalanine–thenardite spectra (Fig. 3(b)) implies that there are competitive gas-phase reactions. This competition results in the self-ionized peaks of phenylalanine being completely suppressed. However, there is also an absence of cation-attached peaks of phenylalanine, which would be expected due to the presence of thenardite. The absence of cation-attached peaks associated with phenylalanine may also be the result of the low binding energy of Na^+ with the phenyl ring as well as with the carbonyl oxygen and the nitrogen of the amine group (Dunbar 2000; Ryzhov *et al*. 2000). Binding energies associated with the aromatic amino acids tend to decrease with decreasing polarization of the aromatic ring, although the stability of Na^+ chelation with phenylalanine is largely controlled by the carbonyl oxygen and/or amine nitrogen (Ryzhov *et al*. 2000). It follows that cation affinity associated with tryptophan will be greater than tyrosine and even more so than phenylalanine. This is further supported by collision-induced dissociation experiments showing that Na^+ tends to form stronger bonds with phenol than with benzene rings (Armentrout & Rodgers 2000), which is contradictory to

https://doi.org/10.1017/S1473550409990231 Published online by Cambridge University Press

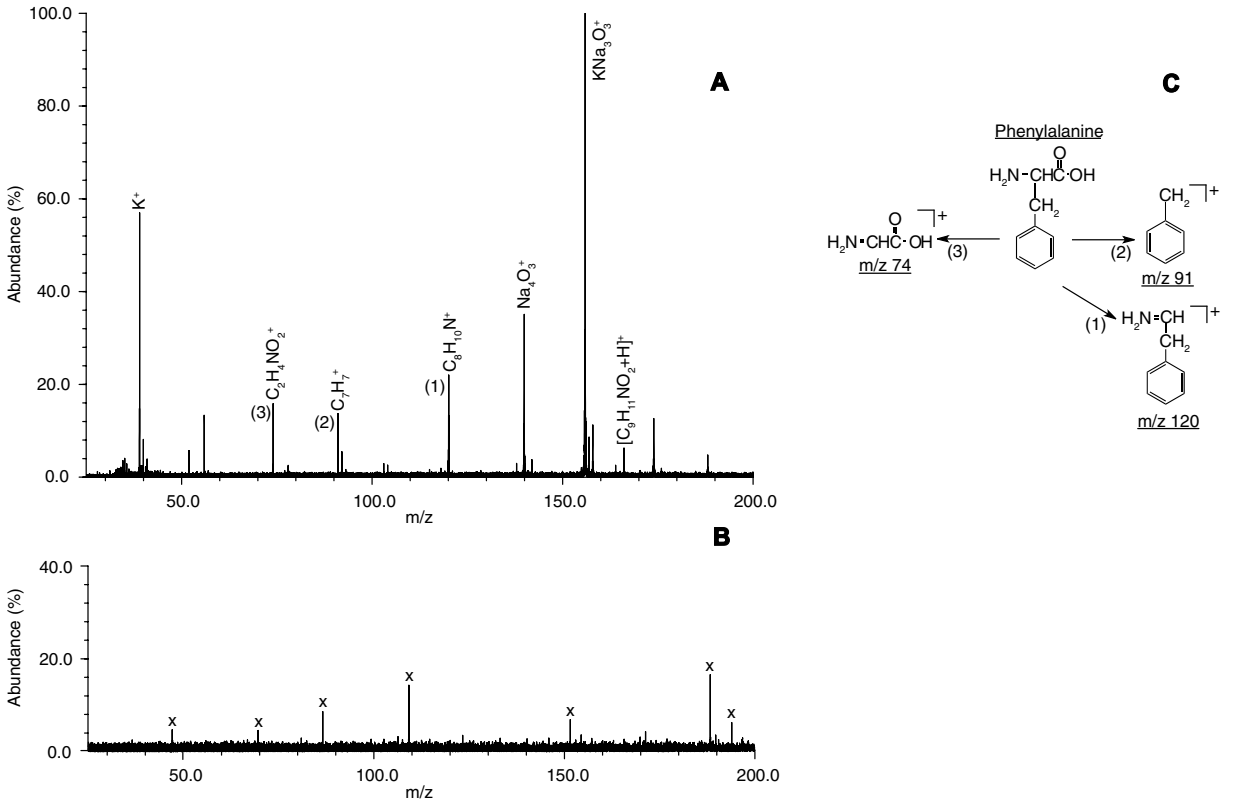

Fig. 3. GALDI-FTICR-MS spectra showing (a) phenylalanine alone and (b) thenardite mixed with phenylalanine (3 ppb). The numbers next to the peaks on (a) correspond to the possible fragmentation ion illustrated in scheme (c). Inorganic cluster ions are designated by ×'s. Structures shown in (c) are not indicative of the actual gas-phase structure, but are shown as a reference to the neutral phenylalanine structure.

studies by Ryzhov *et al.* (2000) and Dunbar (2000) that suggest Na^+ binds to phenol and benzene rings with equal strength. Even though phenylalanine is less prone to cationization than tyrosine or tryptophan, cation attachment can occur when the laser intensity is near the optimized peak height irradiances of singly-charged alkali element ions (Karas *et al.* 1985). At these irradiances, the alkali element ions and cation-attached peaks have comparable peak heights, but at higher intensities alkali element ion formation dominates, while cation-attached abundances decrease (Karas *et al.* 1985). This observation is concurrent with the peak heights of the singly charged K^+ ions and alkali element-attached inorganic cluster ions in Fig. 3(a). Thus, the absence of Na-attachment peaks in Fig. 3(b) could reflect both the low cation binding energy of phenylalanine and the typical laser intensity used in this study, while the absence of self-ionized peaks in Fig. 3(b) may result from thenardite suppressing the self-ionization mechanisms of phenylalanine. The exact mechanisms are still unclear, but could reflect the suppression of ion formation or that the self-ionization occurs, but is subsequently neutralized in the desorption plume due to their interaction with desorption products from thenardite.

The major peak of the tyrosine spectrum (Fig. 4(a)) is observed at m/z 107 ($C_7H_7O^+$), which is consistent with previous tyrosine spectra (Vorsa *et al.* 1999; Plekan *et al.* 2008). The $C_7H_7O^+$ ions arise from fragmentation of the C_α—C_β bond and the concomitant loss of the H^+ ion from the attached hydroxyl group (Fig. 4(c)). The additional loss of the O from the $C_7H_7O^+$ ion leads to the $C_7H_7^+$ fragment ion (m/z 91). Fragmentation of the molecular backbone (Fig. 4(c)) is observed by successive cleaving of the amine group ([M-NH_2]) and the carboxyl group ([M-COOH]) at m/z 165 and 136, respectively. This fragmentation is consistent with previous tyrosine spectra (Vorsa *et al.* 1999). Both fragments are less than 10% of the major peak and comparable in intensity to the molecular ion at m/z 182.

Structurally, tyrosine is identical to phenylalanine with the addition of a hydroxyl group bonded to the aromatic ring. Although this hydroxyl group is located far from the C_α—C_β bond, the tyrosine spectrum is much different than the phenylalanine spectrum. This dichotomy results from the ionization energy potentials and the preferential organization of the positive charge after cleavage of the C_α—C_β bond. For tyrosine, the lowest ionization energy is attributed to the removal of the π-electron from the phenol functional group; this differs from phenylalanine where the lowest ionization energy corresponds to removal of the amine-group electron or the phenyl-group electron (Campbell *et al.* 1992; McLafferty & Tureček 1993). As a result, the positive charge in tyrosine is transferred to the C_β fragment (phenol ring)

https://doi.org/10.1017/S1473550409990231 Published online by Cambridge University Press

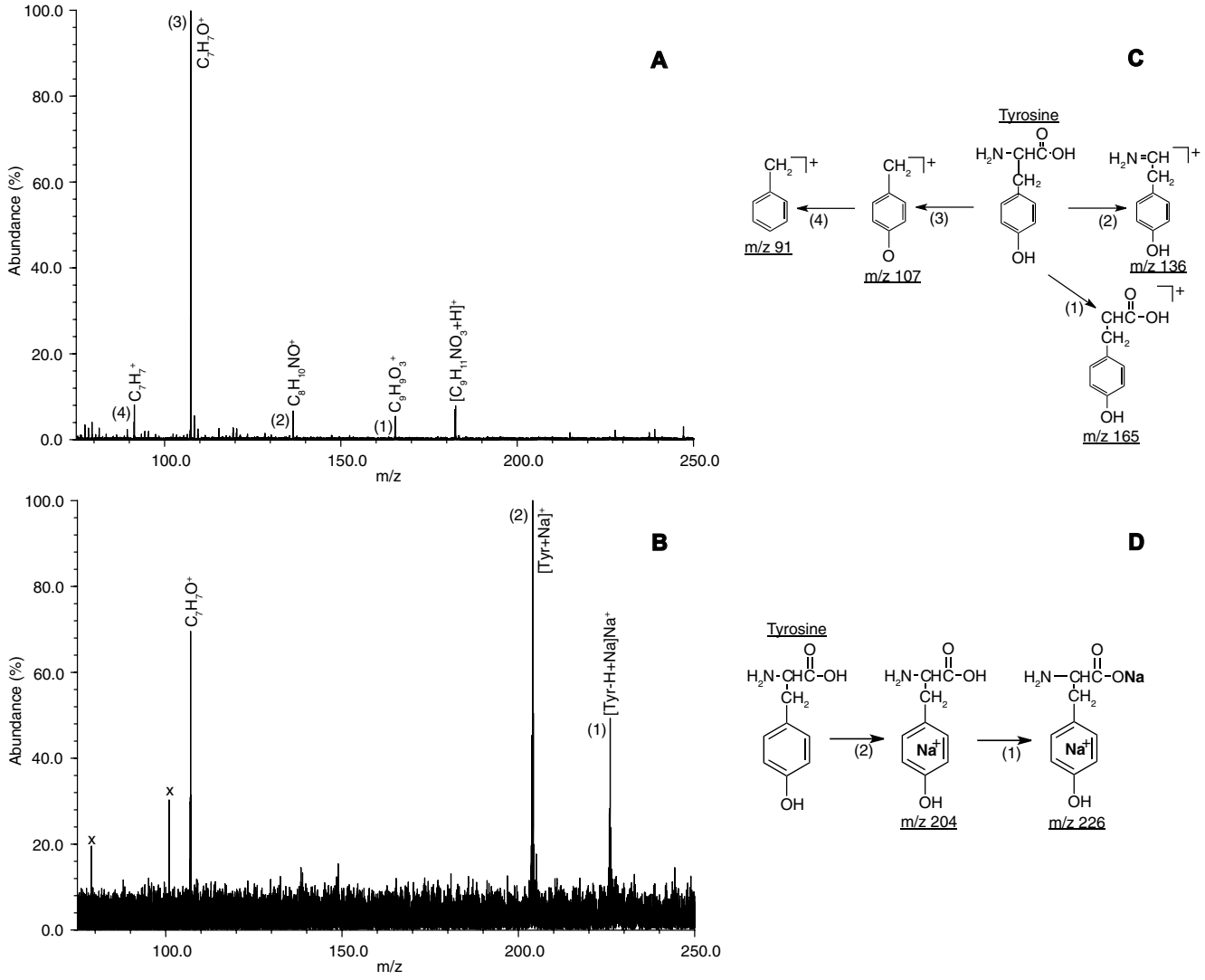

Fig. 4. GALDI-FTICR-MS spectra showing (a) tyrosine alone and (b) thenardite mixed with tyrosine (3 ppb). The numbers next to the peaks on (a) correspond to the possible fragmentation ion illustrated in scheme (c). Likewise values on (b) correspond to the possible fragmentation ion illustrated in scheme (d). Inorganic cluster ions are designated by ×'s. Structures shown in (c) and (d) are not indicative of the actual gas-phase structure, but are shown as a reference to the neutral tyrosine structure.

(Willey *et al.* 1998; Plekan *et al.* 2008). Conversely, for phenylalanine the relocation of the positive charge is dominated by the C_α fragment. This preferential charge localization in tyrosine along with the subsequent hydroxyl deprotonation from the phenol group leads to the formation of the $C_7H_7O^+$ major peak. The presence of this peak suggests that thenardite does not significantly affect the $C_7H_7O^+$ formation mechanism. Conversely, the self-ionization peaks in the phenylalanine spectrum are suppressed and absent when phenylalanine is associated with thenardite.

Unlike the corresponding phenylalanine spectrum, the spectrum of tyrosine mixed with thenardite (Fig. 4(b)) is virtually devoid of inorganic cluster ions, although inorganic cluster ions were observed in other spectra from the same sample. This discrepancy is not unusual considering the single-shot technique and the heterogeneity of the sample. Additionally, it is possible that inorganic cluster ion formation may be affected by the relative amount of organic constituent present in a particular shot. However, only a small number of peaks are typically observed in the spectra, which are either from tyrosine fragmentation or cation attachment between thenardite and tyrosine (Fig. 4(d)). An exception is found in the peaks at m/z 78 and 100, which represent inorganic cluster ions based on their mass defect, similar to peaks found in previous spectra of Na-sulphates (Van Vaeck *et al.* 1998; Richardson *et al.* 2008). It is likely that the presence of the organic analyte affects the production of the inorganic peaks from thenardite, possibly through alterations of the desorption process or through competitive gas-phase reactions.

The major peak in spectra from the tyrosine mixed with thenardite samples (Fig. 4(b)) corresponds to Na^+ binding to the π-electron from the aromatic ring of tyrosine (Fig. 4(d)). This Na-π bond is likely to be centred across the face of the

https://doi.org/10.1017/S1473550409990231 Published online by Cambridge University Press

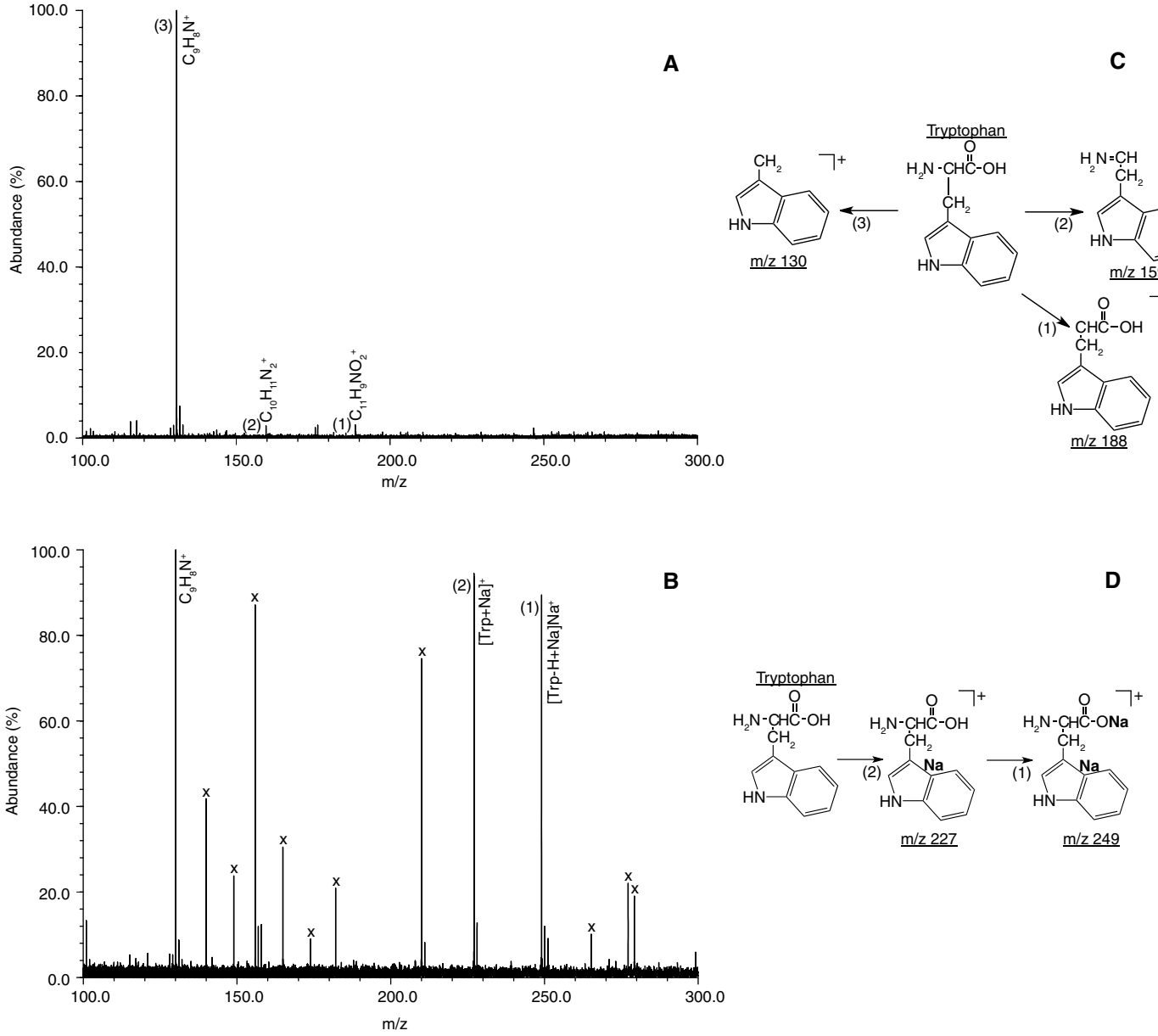

Fig. 5. GALDI-FTICR-MS spectra showing (a) tryptophan alone and (b) thenardite mixed with tryptophan (3 ppb). The numbers next to the peaks on (a) correspond to the possible fragmentation ion illustrated in scheme (c). Likewise values on (b) correspond to the possible fragmentation ion illustrated in scheme (d). Inorganic cluster ions are designated by ×'s. Structures shown in (c) and (d) are not indicative of the actual gas-phase structure, but are shown as a reference to the neutral tryptophan structure.

aromatic ring with chelation by the phenol ring as well as the amine nitrogen and carbonyl oxygen (Ryzhov *et al*. 2000). An additional sodium exchanges with the hydrogen of the carboxyl group to form the alkaline carboxylate salt, either in the condensed phase or in a gas-phase reaction, leading to formation of $[M\text{-}H + Na]Na^+$ ions observed at m/z 226 with a peak height roughly half that of the single cation-attached peak. An ion with two alkali metals attached is sometimes referred to as a double-cation attached ion (Tomlinson *et al*. 1999; Lou *et al*. 2007), which is a slight misnomer because only one of the alkali metals is providing the charge for the singly charged ion.

The structure of tryptophan is characterized by the indole functional group: a benzene ring attached to an N-heterocyclic five-member ring (pyrrole). The major peak (m/z 130) of the tryptophan spectrum (Fig. 5(a)) is attributed to the dehydroindole ion ($C_9H_8N^+$). This major peak is consistent with previous studies of tryptophan mass spectra (Junk & Svec 1963; Vorsa *et al*. 1999; Wilson *et al*. 2006; Plekan *et al*. 2008). Fragmentation of the molecular backbone (Fig. 5(c)) is evident as loss of the amine group ($[M\text{-}NH_2]$) at m/z 188, similar to previous observations using LDMS (Karas *et al*. 1985; Wilson *et al*. 2006; Gogichaeva *et al*. 2007), and time-of-flight secondary ion mass spectrometry techniques (Vorsa *et al*. 1999). Additional fragmentation of the molecular backbone is seen at m/z 159, corresponding to decarboxylation.

Figure 5(b) shows a spectrum of thenardite mixed with tryptophan. The major peak in the spectrum, as with the tryptophan spectrum, corresponds to the dehydroindole ion at m/z 130. Simple cation attachment $[M + Na]^+$ is observed at m/z 227, corresponding to a Na^+ ion attaching to the indole functional group (Fig. 5(d)). Further gas-phase reactions between tryptophan and thenardite lead to the formation of the double cation-attached ion ($[M\text{-}H + Na]Na^+$) observed at m/z 249 (Fig. 5(d)). This peak is roughly 80% of the major peak and slightly less abundant than the $[M + Na]^+$ peak.

As previously mentioned, Na^+ has the strongest affinity to bind with tryptophan, evidenced by the presence and high abundance of both the single and double cation-attached peaks in Fig. 5(b). The formation of the double cation-attached peak (m/z 249) is accomplished via a multiple step process (Fig. 5(d)). Initially, a Na^+ ion attaches to the π-electron of the indole aromatic ring. This attachment is likely to be offset to the side of the pyrrole ring face, rather than the benzene ring, because of differences in binding energies between the two regions of the indole group. This offset position above the pyrrole ring results in cation chelation to the nitrogen from the amine group, the oxygen from the carbonyl group, and the π-electrons from the pyrrole group (Ryzhov *et al*. 2000). Secondly, another Na^+ from thenardite replaces the H^+ ion from the carboxyl group, either in the desorption plume or in the gas phase, leading to the formation of the $[M + Na\text{-}H]Na^+$ ion (Yan *et al*. 2007b). Comparison of the tyrosine and tryptophan spectra, with and without thenardite present, suggests that cation attachment competes with and suppresses the self-ionization mechanisms and some related fragmentation pathways. However, fragment peaks related to the aromatic side chains of tyrosine and tryptophan are still observed in the presence of thenardite.

Other minerals can also provide cations to function in a similar manner to thenardite for ionizing bio/organic compounds. Sodium ions from the mineral halite (NaCl) participate in the formation of cation-attached peaks associated with the amino acids histidine, threonine and cysteine (Yan *et al*. 2007b). These results are not surprising considering the ease with which Na^+ ionizes and its affinity to interact with bio/organic compounds in the desorption plume or gas phase (Liu *et al*. 2001); however, it is interesting to note that high concentrations of salts, similar to the minerals halite and thenardite, suppress ion formation in MALDI (Goheen *et al*. 1997; Yao *et al*. 1998). Cation attachment to histidine (Yan *et al*. 2007b) is not surprising, considering the aromaticity and the high alkali affinity of histidine (Kish *et al*. 2003). Thus, cation-attachment mechanisms of histidine with halite are likely to be similar to that described above for tyrosine and tryptophan in the presence of thenardite. As threonine and cysteine are aliphatic amino acids, the formation of their cation-attached peaks is likely to be different than their aromatic counterparts. Regardless of the formation mechanisms, the occurrence of cation-attached peaks associated with different Na-salt geomatrices (halide and sulphate) suggests that Na^+ ionization and subsequent gas-phase interactions are common, regardless of the anion or oxyanion moiety.

Conclusions

Pure samples of the aromatic amino acids (phenylalanine, tyrosine and tryptophan) all produce ions through self-ionization mechanism(s) and produce similar fragmentation patterns when thenardite is absent. In all spectra, the fragmentation of the molecular backbone is observed by loss of the carboxyl group. Spectra from tyrosine and tryptophan show additional loss of the amine group. Further, fragmentation is observed in aromatic side chains, which accounts for the major peaks in the tyrosine and tryptophan spectrum, which is consistent with ionization potentials between the aromatic ring and the molecular backbone.

Of the aromatic amino acids used in this study, tyrosine and tryptophan associated with thenardite are observed to undergo cationization. The cation attachment results from the high affinity of the aromatic side chain for binding with alkali metal ions. Substitution of the carboxyl hydrogen by Na leads to formation of 'double cation-attached' ions. In contrast, phenylalanine shows no evidence of Na^+ interaction, a consequence of system parameters (e.g. laser intensity, wavelength) and/or lower alkali element-binding energy. In addition, the presence of thenardite suppresses all of the self-ionized peaks that are definitive for the presence of phenylalanine, leaving only fragment peaks common to all three aromatic amino acids studied. However, the ability of cation attachment to out-compete and suppress the majority of the self-ionized peaks for tyrosine and tryptophan associated with thenardite makes interpretation of spectra for these aromatic amino acids less complicated.

https://doi.org/10.1017/S1473550409990231 Published online by Cambridge University Press

The effectiveness of thenardite, and other Na-related geomatrices, for detection of bio/organic compounds is a product of analyte–matrix interactions and competitive gas-phase reactions. Understanding these types of Na–sulphate mineral and bio/organic compound interactions has astrobiological implications because terrestrial Na–sulphate mineral deposits are known to harbour bio/organic compounds; therefore, the presence of these minerals on Mars and Europa represents a prime opportunity to search for signs of life using LDMS instruments on rovers.

Acknowledgments

The authors acknowledge support from the National Aeronautics and Space Agency (NASA) Exobiology Program (NNX08AP59G). CDR would also like to thank Montana Space Grant Consortium for support. Research performed at the Idaho National Laboratory under DOE Idaho Operations Office Contract DE-AC07-05ID14517.

References

Armentrout, P.B. & Rodgers, M.T. (2000). An absolute sodium cation affinity scale: Threshold collision-induced dissociation experiments and ab initio theory. *J. Phys. Chem.* **104**, 2238–2247.

Aubrey, A., Cleaves, H.J., Chalmers, J.H., Skelley, A.M., Mathies, R.A., Grunthaner, F.J., Ehrenfreund, P. & Bada, J.L. (2006). Sulfate minerals and organic compounds on Mars. *Geology* **34**, 357–360.

Aubriet, F. (2007). Laser-induced Fourier transform ion cyclotron resonance mass spectrometry of organic and inorganic compounds: Methodologies and applications. *Anal. Bioanal. Chem.* **389**, 1381–1396.

Aubriet, F., Carre, V. & Muller, J.F. (2005). Laser desorption and laser ablation Fourier transform mass spectrometry for the analysis of pollutants in complex matrices. *Spectrosc. Eur.* **17**, 14–22.

Aubriet, F. & Muller, J. (2008). Laser ablation mass spectrometry of inorganic transition metal compounds. *Am. Soc. Mass Spectrom.* **19**, 488–501.

Budimir, N., Blais, J.C., Fournier, T. & Tabet, J.C. (2007). Desorption/ionization on porous silicon mass spectrometry (DIOS) of model cationized fatty acids. *J. Mass Spectrom.* **42**, 42–48.

Campbell, S., Beauchamp, J., Rempe, M. & Lichtenberger, D. (1992). Correlations of lone pair ionization energies with proton affinities of amino acids and related compounds. Site specificity or protonation. *Int. J. Mass Spectrom. Ion Processes* **117**, 83–99.

Chela-Flores, J. (2006). The sulphur dilemma: Are there biosignatures on Europa's icy and patchy surface? *Int. J. Astrobiol.* **5**, 17–22.

Chyba, C. & McDonald, G. (1995). The origin of life in the solar system: Current issues. *Annu. Rev. Earth Planet. Scie.* **23**, 215–249.

Chyba, C. & Phillips, C. (2002). Europa as an abode of life. *Orig. Life Evol. Biosph.* **32**, 47–67.

Comisarow, M.B. (1993). Fundamental aspects of FT-ICR and applications to chemistry. *Hyperfine Interact.* **81**, 171–178.

Dunbar, R. (2000). Complexation of Na^+ and K^+ to aromatic amino acids: A density functional computational study of cation-interaction. *J. Phys. Chem.* **104**, 8067–8074.

El Aribi, H., Orlova, G., Hopkinson, A. & Siu, K. (2004). Gas-phase fragmentation reactions of protonated aromatic amino acids: concomitant and consecutive neutral eliminations and radical cation formation. *J. Phys. Chem. A* **108**, 3844–3853.

Evans-Nguyen, T., Becker, L., Doroschenko, V. & Cotter, R. (2008). Development of a low power, high mass range mass spectrometer for Mars surface analysis. *Int. J. Mass Spectrom.* **278**, 170–177.

Fanale, F.P., Li, Y.-H., De Carlo, E., Farley, C., Sharma, S.K., Horton, K. & Granahan, J.C. (2001). An experimental estimate of Europa's "ocean" composition independent of Galileo orbital remote sensing. *J. Geophys. Res.* **106**, 14 595–14 600.

Gaidos, E., Nealson, K. & Kirschvink, J. (1999). Life in ice-covered oceans. *Science* **284**, 1631–1633.

Gogichaeva, N.V., Williams, T. & Alterman, M.A. (2007). MALDI TOF/TOF tandem mass spectrometry as a new tool for amino acid analysis. *J. Am. Soc. Mass Spectrom.* **18**, 279–284.

Goheen, S.C., Wahl, K.L., Campbell, J.A. & Hess, W.P. (1997). Mass spectrometry of low molecular mass solids by matrix-assisted laser desorption/ionization. *J. Mass Spectrom.* **32**, 820–828.

Ham, J.E., Durham, B. & Scott, J.R. (2003). Comparison of laser desorption and matrix-assisted laser desorption/ionization for ruthenium and osmium trisbipyridine complexes using Fourier transform mass spectrometry. *J. Am. Soc. Mass Spectrom.* **14**, 393–400.

Hill, C. & Forti, P. (1997). *Cave Minerals of the World.* National Speleological Society, Huntsville, AL.

Johnson, R.E. (2000). Sodium at Europa. *Icarus* **143**, 429–433.

Junk, G. & Svec, H. (1963). The mass spectra of the a-amino acids. *J. Am. Chem. Soc.* **85**, 839.

Karas, M., Bachmann, D. & Hillenkamp, F. (1985). Influence of the wavelength in high-irradiance ultraviolet laser desorption mass spectrometry of organic molecules. *Anal. Chem.* **57**, 2935–2939.

Karas, M. & Hillenkamp, F. (1988). Laser desorption ionization of proteins with molecular masses exceeding 10000 daltons. *Anal. Chem.* **60**, 2299–2301.

Kargel, J.S., Kaye, J.Z., Head, J.W.I., Marion, G.M., Sassen, R., Crowly, J.K., Ballesteros, O.P., Grant, S.A. & Hogenboom, D.L. (2000). Europa's crust and ocean: origin, composition, and the prospects for life. *Icarus* **148**, 226–265.

Karlo, J.H., Jorgenson, D.B. & Shineldecker, C.L. (1980). Sulfate minerals in snake river plain volcanoes. *Northwest Sci.* **54**, 178–182.

Kim, S., Rodgers, R.P. & Marshall, A.G. (2006). Truly "exact" mass: Elemental composition can be determined uniquely from molecular mass measurement at similar to 0.1 mDa accuracy for molecules up to similar to 500 Da. *Int. J. Mass Spectrom.* **251**, 260–265.

Kish, M., Ohanessian, G. & Wesdemiotis, C. (2003). The Na^+ affinities of a-amino acid: Side-chain substituent effects. *Int. J. Mass Spectrom.* **227**, 509–524.

Klein, H. (1979). Viking mission and the search for life on Mars. *Rev. Geophys.* **17**, 1655–1662.

Knochenmuss, R., Dubois, F., Dale, M.J. & Zenobi, R. (1996). The matrix suppression effect and ionization mechanisms in matrix-assisted laser desorption/ionization. *Rapid Commun. Mass Spectrom.* **10**, 871–877.

Kotler, J.M., Hinman, N.W., Yan, B., Stoner, D.L. & Scott, J.R. (2008). Glycine Identification in natural jarosites using laser-desorption Fourier transform mass spectrometry: Implications for the search for life on Mars. *Astrobiology* **8**, 253–266.

Kotler, J.M., Richardson, C.D., Hinman, N.W. & Scott, J.R. (2009). The stellar stew: Distribution of extraterrestrial organic compounds in the universe. In *From Simple Molecules to primitive life*, ed. Basiuk, V.A., pp. in press. American Scientific Publishers, Valencia, CA.

Liu, J., Tseng, K. & Lebrilla, C.B. (2001). A new external ionization multisample MALDI source for Fourier transform mass spectrometry. *Int. J. Mass Spectrom.* **204**, 23–29.

Lou, X., Sinkeldam, R., van Houts, W., Nicolas, Y., Janssen, P., van Dongen, J., Vekemans, J. & Meijer, E. (2007). Double cation adduction in matrix-assisted laser desorption/ionization time-of-flight mass spectrometry of electron deficient anthraquinone derivatives. *J. Mass Spectrom.* **42**, 293–303.

Mangold, N., Gendrin, A., Gondet, B., LeMouelic, S., Quantin, C., Ansan, V., Bibring, J., Langevin, Y., Masson, P. & Neukum, G. (2008). Spectral and geological study of the sulfate-rich region of West Candor Chasma, Mars. *Icarus* **194**, 519–543.

Marshall, A.G. & Hendrickson, C.L. (2002). Fourier transform ion cyclotron resonance detection: principles and experimental configurations. *Int. J. Mass Spectrom.* **215**, 59–75.

Marshall, A.G., Hendrickson, C.L. & Jackson, G.S. (1998). Fourier transform ion cyclotron resonance mass spectrometry: A primer. *Mass Spectrom. Rev.* **17**, 1–35.

McCord, T.B. *et al.* (1998). Salts on Europa's surface detected by Galileo's near infrared mapping spectrometer. *Science* **280**, 1242–1245.

McCord, T.B., Hansen, G.B. & Hibbitts, C.A. (2001). Hydrates salt minerals on Ganymede's surface: Evidence of an ocean below. *Science* **292**, 1523–1525.

McCord, T.B. *et al.* (1999). Hydrated salt minerals on Europa's surface from the Galileo near-infrared mapping spectrometer (NIMS) investigation. *J. Geophys. Res.* **104**, 11 827–11 851.

McJunkin, T.R., Tremblay, P.L. & Scott, J.R. (2002). Automation and control of an imaging internal laser desorption Fourier transform mass spectrometer (I²LD-FTMS). *Journal of the Association for Laboratory Automation* **7**, 76–83.

McKay, C.P. (2007). An approach to searching for life on Mars, Europa, and Enceladus. *Space Sci. Rev.* **135**, 49–54.

McLafferty, F.W. & Tureček, F. (1993). *Interpretation of Mass Spectra.* University Science Books, Sausalito, CA.

Ohno, H., Igarashi, M. & Hondoh, T. (2006). Characteristics of salt inclusions in polar ice from Dome Fuji, East Antarctica. *Geophys. Res. Lett.* **33**, L08501.1–L08501.5.

Orlando, T.M., McCord, T.B. & Grieves, G.A. (2005). The chemical nature of Europa surface material and the relation to a subsurface ocean. *Icarus* **177**, 528–533.

Oro, J. (1979). Viking mission and the question of life on Mars- introduction. *J. Mol. Evol.* **14**, 3–4.

Parnell, J., Cullen, D., Sims, M., Bowden, S., Cockell, C., Court, R., Ehrenfreund, P., Gaubert, F., Grant, W., Parro, V., Rohmer, M., Sephton, M., Stan-Lotter, H., Steele, A., Toporski, J., Vago, J. (2007). Searching for Life on Mars: Selection of Molecular Targets for ESA's Aurora ExoMars Mission. *Astrobiology* **7**, 578–604.

Plekan, O., Feyer, V., Richter, R., Coreno, M. & Prince, K.C. (2008). Valence photoionization and photofragmentation of aromatic amino acids. *Mol. Phys.* **106**, 1143–1153.

Porat, I., Waters, B.W., Teng, Q. & Whitman, W.B. (2004). Two biosynthetic pathways for aromatic amino acids in the archaeon *Methanococcus maripaludis*. *J. Bacteriol.* **186**, 4940–4950.

Rankin, A.M., Wolff, E.W. & Martin, S. (2002). Frost flowers: Implicatoins for tropospheric chemistry and ice core interpretation. *J. Geophys. Res.* **107**, 4683.

Richardson, C.D., Hinman, N.W., McJunkin, T.R., Kotler, J.M. & Scott, J.R. (2008). Exploring biosignatures associated with thenardite by geomatrix-assisted laser desorption/ionization Fourier transform ion cyclotron resonance mass spectrometry (GALDI-FTICR-MS). *Geomicrobiol. J.* **25**, 432–440.

Ryzhov, V., Dunbar, R.C., Cerda, B. & Wesdemiotis, C. (2000). Cation-π effects in the complexation of Na^+ and K^+ with Phe, Tyr, and Trp in the gas phase. *Am. Soc. Mass Spectrom.* **11**, 1037–1046.

Sack, T.M., Lapp, R.L., Gross, M.L. & Kimble, B.J. (1984). A method for the statistical evaluation of accurate mass measurement quality. *Int. J. Mass Spectrom. Ion Processes* **61**, 191–213.

Scott, J.R., McJunkin, T.R. & Tremblay, P.L. (2003). Automated analysis of mass spectral data using fuzzy logic classification. *Journal of the Association for Laboratory Automation* **8**, 61–63.

Scott, J.R. & Tremblay, P.L. (2002). Highly reproducible laser beam scanning device for an internal source laser desorption microprobe Fourier transform mass spectrometer. *Rev. Sci. Instrum.* **73**, 1108–1116.

Scott, J.R., Yan, B. & Stoner, D.L. (2006). Spatially correlated spectroscopic analysis of microbe-mineral interactions. *J. Microbiol Methods* **67**, 381–384.

Squyres, S.W. *et al.* (2004). The Opportunity rover's Athena science investigation at Meridiani Planum, Mars. *Science* **306**, 1698–1703.

Storrie-Lombardi, M.C., Hug, W.F., McDonald, G.D., Tsapin, A.I. & Nealson, K.H. (2001). Hollow cathode ion lasers for deep ultraviolet Raman spectroscopy and fluorescence imaging. *Rev. Sci. Instrum.* **72**, 4452–4459.

Tomlinson, M., Scott, J., Wilkins, C., Wright, J. & White, W. (1999). Fragmentation of an alkali metal-attached peptide probed by collision-induced dissociation Fourier transform mass spectrometry and computational methodology. *J. Mass Spectrom.* **34**, 958–968.

Tosca, N.J. & McLennan, S.M. (2006). Chemical divides and evaporite assemblages on Mars. *Earth Planet. Sci. Lett.* **241**, 21–31.

Van Vaeck, L., Adriaens, A. & Adams, F. (1998). Microscopical speciation analysis with laser microprobe mass spectrometry and static secondary ion mass spectrometry. *Spectrochim Acta, Part B* **53**, 367–378.

Vorsa, V., Kono, T., Willey, K. & Winograd, N. (1999). Femtosecond photoionization of ion beam desorbed aliphatic and aromatic amino acids: fragmentation via alpha-cleavage reactions. *J. Phys. Chem. B* **106**, 7889–7895.

Wiens, R.C., Burnett, D.S., Calaway, W.F., Hansen, C.S., Lykke, K.R. & Pellin, M.J. (1997). Sputtering products of sodium sulfate: Implications for Io's surface and for sodium-bearing molecules in the Io torus. *Icarus* **128**, 386–397.

Willey, K., Vorsa, V., Braun, R. & Winograd, N. (1998). Postionization of molecules desorbed from surfaces by keV ion bombardment with femtosecond laser pulses. *Rapid Commun. Mass Spectrom.* **12**, 1253–1260.

Wilson, K.R., Jimenez-Cruz, M., Nicolas, C., Belau, L., Leone, S.R. & Ahmed, M. (2006). Thermal vaporization of biological nanoparticles: fragment-free vacuum ultraviolet photoionization mass spectra of tryptophan, phenylalanine-glycine-glycine, and B-carotene. *J. Phys. Chem. A* **110**, 2106–2113.

Yan, B., Stoner, D.L., Kotler, J.M., Hinman, N.W. & Scott, J.R. (2007a). Detection of biosignatures by geomatrix-assisted laser desorption/Ionization (GALDI) mass spectrometry. *Geomicrobiol.* **24**, 379–385.

Yan, B., Stoner, D.L. & Scott, J.R. (2007b). Direct LD-FTMS detection of mineral-associated PAHs and their influence on the detection of other organics. *Talanta* **72**, 634–641.

Yao, J., Scott, J.R., Young, M.K. & Wilkins, C.L. (1998). Importance of matrix : analyte ratio for buffer tolerance using 2,5-dihydroxybenzoic acid as a matrix in matrix-assisted laser desorption/ionization Fourier transform mass spectrometry and matrix-assisted laser desorption/ionization time of flight. *J. Am. Soc. Mass Spectrom.* **9**, 805–813.

Zhu, M., Xie, H., Guan, H. & Smith, R. (2006). Mineral and lithologic mapping of martian low albedo regions using OMEGA data. In *Lunar and Planetary Science XXXVII*, pp. 2173.

Zolotov, M.Y. & Shock, E.L. (2001). Composition and stability of salts on the surface of Europa and their oceanic origin. *J. Geophys. Res.* **106**, 32 815–32 827.